Proceedings

of the

XXVI Congreso de Ecuaciones Diferenciales y Aplicaciones
XVI Congreso de Matemática Aplicada

Gijón (Asturias), Spain

June 14-18, 2021

CEDYA CMA 2020 GIJÓN

SēMA
Sociedad Española de Matemática Aplicada

Universidad de Oviedo

Editors:
Rafael Gallego, Mariano Mateos

Universidad de Oviedo
Servicio de Publicaciones de la Universidad de Oviedo
Campus de Humanidades. Edificio de Servicios. 33011 Oviedo (Asturias)
Tel. 985 10 95 03 Fax 985 10 95 07
http: www.uniovi.es/publicaciones
servipub@uniovi.es

ISBN: 978-84-18482-21-2

Foreword

It is with great pleasure that we present the Proceedings of the 26th Congress of Differential Equations and Applications / 16th Congress of Applied Mathematics (XXVI CEDYA / XVI CMA), the biennial congress of the Spanish Society of Applied Mathematics S$\vec{e}$MA, which is held in Gijón, Spain from June 14 to June 18, 2021.

In this volume we gather the short papers sent by some of the almost three hundred and twenty communications presented in the conference. Abstracts of all those communications can be found in the abstract book of the congress. Moreover, full papers by invited lecturers will shortly appear in a special issue of the S$\vec{e}$MA Journal.

The first CEDYA was celebrated in 1978 in Madrid, and the first joint CEDYA / CMA took place in Málaga in 1989. Our congress focuses on different fields of applied mathematics: Dynamical Systems and Ordinary Differential Equations, Partial Differential Equations, Numerical Analysis and Simulation, Numerical Linear Algebra, Optimal Control and Inverse Problems and Applications of Mathematics to Industry, Social Sciences, and Biology. Communications in other related topics such as Scientific Computation, Approximation Theory, Discrete Mathematics and Mathematical Education are also common.

For the last few editions, the congress has been structured in mini-symposia. In Gijón, we will have eighteen minis-symposia, proposed by different researchers and groups, and also five thematic sessions organized by the local organizing committee to distribute the individual contributions. We will also have a poster session and ten invited lectures. Among all the mini-symposia, we want to highlight the one dedicated to the memory of our colleague Francisco Javier “Pancho” Sayas, which gathers two plenary lectures, thirty-six talks, and more than forty invited people that have expressed their wish to pay tribute to his figure and work.

This edition has been deeply marked by the COVID-19 pandemic. First scheduled for June 2020, we had to postpone it one year, and move to a hybrid format. Roughly half of the participants attended the conference online, while the other half came to Gijón. Taking a normal conference and moving to a hybrid format in one year has meant a lot of efforts from all the parties involved. Not only did we, as organizing committee, see how much of the work already done had to be undone and redone in a different way, but also the administration staff, the scientific committee, the mini-symposia organizers, and many of the contributors had to work overtime for the change.

Just to name a few of the problems that all of us faced: some of the already accepted mini-symposia and contributed talks had to be withdrawn for different reasons (mainly because of the lack of flexibility of the funding agencies); it became quite clear since the very first moment that, no matter how well things evolved, it would be nearly impossible for most international participants to come to Gijón; reservations with the hotels and contracts with the suppliers had to be cancelled; and there was a lot of uncertainty, and even anxiety could be said, until we were able to confirm that the face-to-face part of the congress could take place as planned.

On the other hand, in the new open call for scientific proposals, we had a nice surprise: many people that would have not been able to participate in the original congress were sending new ideas for mini-symposia, individual contributions and posters. This meant that the total number of communications was about twenty percent greater than the original one, with most of the new contributions sent by students.

There were almost one hundred and twenty students registered for this CEDYA / CMA. The hybrid format allows students to participate at very low expense for their funding agencies, and this gives them the opportunity to attend different conferences and get more merits. But this, which can be seen as an advantage, makes it harder for them to obtain a full conference experience. Alfréd Rényi said: “a mathematician is a device for turning coffee into theorems”. Experience has taught us that a congress is the best place for a mathematician to have a lot of coffee. And coffee cannot be served online.

In Gijón, June 4, 2021

The Local Organizing Committee from the Universidad de Oviedo

Scientific Committee

- Juan Luis Vázquez, Universidad Autónoma de Madrid
- María Paz Calvo, Universidad de Valladolid
- Laura Grigori, INRIA Paris
- José Antonio Langa, Universidad de Sevilla
- Mikel Lezaun, Euskal Herriko Unibersitatea
- Peter Monk, University of Delaware
- Ira Neitzel, Universität Bonn
- JoséÁngel Rodríguez, Universidad de Oviedo
- Fernando de Terán, Universidad Carlos III de Madrid

Sponsors

- Sociedad Española de Matemática Aplicada
- Departamento de Matemáticas de la Universidad de Oviedo
- Escuela Politécnica de Ingeniería de Gijón
- Gijón Convention Bureau
- Ayuntamiento de Gijón

Local Organizing Committee from the Universidad de Oviedo

- Pedro Alonso Velázquez
- Rafael Gallego
- Mariano Mateos
- Omar Menéndez
- Virginia Selgas
- Marisa Serrano
- Jesús Suárez Pérez del Río

Contents

XXVI Congreso de Ecuaciones Diferenciales y Aplicaciones
XVI Congreso de Matemática Aplicada
Gijón, 14-18 junio 2021
(pp. 122–129)

Homoclinic bifurcations in the unfolding of the nilpotent singularity of codimension 4 in $\mathbb{R}^4$

Pablo S. Casas[1], **Fátima Drubi**[2], **Santiago Ibáñez**[2]
1. pabloscasas@uniovi.es *Universidad de Oviedo, Spain*
2. *Universidad de Oviedo, Spain*

Abstract

The rich variety of homoclinic phenomena exhibited by the limit family of any generic unfolding of a four-dimensional nilpotent singularity of codimension-four is discussed. Specifically, numerical techniques based on the Taylor integrator and the expansion of the invariant manifolds were designed for this family. A partial bifurcation diagram which includes, besides a suggestive catalogue of local bifurcations of equilibria, folds and period doublings of periodic orbits is also given. These results are certainly the first steps towards a much more ambitious goal: to achieve a general understanding of these codimension-four unfoldings.

1. Introduction

Let X be a C^∞ vector field on $\mathbb{R}^n$ with $X(0) = 0$ and 1-jet at 0 linearly conjugate to $\sum_{i=1}^{n-1} x_{i+1}\,\partial/\partial x_i$. Vector fields satisfying this assumption make up a set of codimension n in the space of germs of singularities in $\mathbb{R}^n$ (see [19] for definitions). As argued in [8], working with appropriate coordinates, X can be written as the following differential equation

$$\left\{\begin{array}{lcll} x_i' &=& x_{i+1} & \text{for} \quad i = 1,\dots,n-1,\\ x_n' &=& f(x), & \end{array}\right.$$

with $x = (x_1,\dots,x_n)$ and $f(x) = O(\|x\|^2)$. We say that 0 (or X itself) is a n-dimensional nilpotent singularity of codimension n when the condition

$$\frac{\partial^2 f}{\partial x_1^2}(0) \neq 0$$

is satisfied.

Consider now a C^∞-family of vector fields X_ν, with $\nu = (\nu_1,\dots,\nu_n) \in \mathbb{R}^n$, such that X_0 is a n-dimensional nilpotent singularity of codimension n. As proved in [8], under generic assumptions, X_ν can be written as follows

$$\left\{\begin{array}{lcll} x_i' &=& x_{i+1} & \text{for} \quad i = 1,\dots,n-1,\\ x_n' &=& \nu_1 + \nu_2 x_2 + \dots + \nu_n x_n + x_1^2 + h(\nu,x), & \end{array}\right.$$

where $\nu_1,\dots,\nu_n$ and the coefficient in front of x_1^2 represent exact coefficients in a Taylor expansion with respect to x and h is of order $O(\|(\nu,x)\|^2)$ and $O(\|(x_2,\dots,x_n)\|^2)$.

As proved in [1], when rescaling parameters and variables by the equations

$$\begin{array}{lcll} \nu_1 &=& \varepsilon^{2n}\bar\nu_1, & \\ \nu_k &=& \varepsilon^{n-k+1}\bar\nu_k & \text{for} \quad k = 2,\dots,n,\\ x_k &=& \varepsilon^{n+k-1}\bar x_k & \text{for} \quad k = 1,\dots,n, \end{array} \tag{1.1}$$

with $\varepsilon > 0$ and $\bar\nu_1^2 + \dots + \bar\nu_n^2 = 1$, X_ν becomes the system

$$\left\{\begin{array}{lcll} \bar x_i' &=& \bar x_{i+1} & \text{for} \quad i = 1,\dots,n-1,\\ \bar x_n' &=& \bar\nu_1 + \bar\nu_2\bar x_2 + \dots + \bar\nu_n\bar x_n + \bar x_1^2 + O(\varepsilon), & \end{array}\right.$$

after division by ε. Variable $\bar x = (\bar x_1,\dots,\bar x_n)$ can be assumed to belong to any arbitrarily large compact in $\mathbb{R}^n$.

Understanding the bifurcation diagram of the limit family ($\varepsilon = 0$) is essential to study the dynamics emerging from the singularity, that is, its unfolding. The limit family when $n = 2$ is a key piece in the study of the Bogdanov-Takens bifurcation ([3,20]). The limit family corresponding to the case $n = 3$ was studied in [11–14]. Among other results, it was proved in [14] that any generic unfolding of the 3-dimensional nilpotent singularity of codimension

3 exhibits strange attractors. Finally, the limit family corresponding to the 4-dimensional nilpotent singularity of codimension four

$$\left\{\begin{array}{lcl} \bar{x}_1' & = & \bar{x}_2, \\ \bar{x}_2' & = & \bar{x}_3, \\ \bar{x}_3' & = & \bar{x}_4, \\ \bar{x}_4' & = & \bar{\nu}_1 + \bar{\nu}_2\bar{x}_2 + \bar{\nu}_3\bar{x}_3 + \bar{\nu}_4\bar{x}_4 + \bar{x}_1^2, \end{array}\right. \tag{1.2}$$

was studied in [1,2,8]. Most notably, it was proved in [1] that any generic unfolding of the singularity contains a bifurcation hypersurface corresponding to bifocal homoclinic orbits. Even so, all the mentioned papers only offer very preliminary results. Consequently, the study of the dynamics exhibited by the limit family in the 4-dimensional case continues to be an interesting and enormous challenge.

In this work we delve into the study of (1.2). In Section 2 we propose directional rescalings that facilitate the study. The numerical methods employed along the paper are described in Section 3. The core of this paper is Section 4 where we provide results related to the existence of homoclinic connections. In addition, a first approximation to the complex structure of bifurcations of periodic orbits displayed in the family is presented in Section 5. We conclude with a brief discussion on related topics of interest.

2. Directional rescalings and reversible case

In what follows, we consider the family (1.2). When $\bar{\nu}_1 > 0$, it can be proven that the function

$$L(\bar{x}_1, \bar{x}_2, \bar{x}_3, \bar{x}_4) = \bar{x}_4 - \bar{\nu}_2\bar{x}_1 - \bar{\nu}_3\bar{x}_2 - \bar{\nu}_4\bar{x}_3$$

is strictly increasing along orbits. Therefore, there are no bounded orbits when $\bar{\nu}_1 > 0$ and the interesting dynamics only emerges for $\bar{\nu}_1 \le 0$. When $\bar{\nu}_1 = 0$, there is a unique equilibrium point at the origin and for $\bar{\nu}_1 < 0$ there exist two equilibrium points at $p_\pm = (\pm\sqrt{-\bar{\nu}_1}, 0, 0, 0)$.

On the other hand, family (1.2) is invariant with respect to the transformation:

$$(\bar{\nu}_1, \bar{\nu}_2, \bar{\nu}_3, \bar{\nu}_4, x_1, x_2, x_3, x_4, t) \longmapsto (\bar{\nu}_1, -\bar{\nu}_2, \bar{\nu}_3, -\bar{\nu}_4, x_1, -x_2, x_3, -x_4, -t).$$

This allows to restrict the study to the case $\bar{\nu}_4 \le 0$. In particular, the divergence of each vector field in the family is given by $\bar{\nu}_4$ so the existence of repellors is not feasible for $\bar{\nu}_4 \leqslant 0$ and attractors also do not exist when $\bar{\nu}_4 = 0$. Additionally, the vector fields are time-reversible when $\bar{\nu}_2 = \bar{\nu}_4 = 0$. As argued in [1,2,8], understanding the dynamics for the subfamily of time-reversible vector fields becomes essential. The dynamics of the linear part is simple around p_+ and richer around p_- (see [1]). The linear part at p_+ always have a pair of real eigenvalues and a pair of complex eigenvalues with non-zero real part. However, the linear part at p_- has

- a double zero eigenvalue and a pair of pure imaginary eigenvalues when $\bar{\nu}_3 = -1$ and $\bar{\nu}_1 = \bar{\nu}_2 = \bar{\nu}_4 = 0$ (we denote this bifurcation point as HBT),
- two double pure imaginary eigenvalues $\pm i(-\bar{\nu}_3/2)^{1/2}$ when $\bar{\nu}_3^2 - 8\sqrt{-\bar{\nu}_1} = 0$, $\bar{\nu}_3 < 0$ and $\bar{\nu}_2 = \bar{\nu}_4 = 0$ (we denote this bifurcation point as HH),
- two double real eigenvalues $\pm(\nu_3/2)^{1/2}$ when $\bar{\nu}_3^2 - 8\sqrt{-\bar{\nu}_1} = 0$, $\bar{\nu}_3 > 0$ and $\bar{\nu}_2 = \bar{\nu}_4 = 0$ (we denote this bifurcation point as BD),
- a double zero eigenvalue and eigenvalues ± 1 when $\bar{\nu}_3 = 1$ and $\bar{\nu}_1 = \bar{\nu}_2 = \bar{\nu}_4 = 0$ (we denote this bifurcation point as BT).

In between bifurcation points HBT and HH on the circumference $\bar{\nu}_1^2 + \bar{\nu}_3^2 = 1$, the linear part at p_- has four pure imaginary eigenvalues $\pm\omega_k i$, with $k = 1, 2$, and $\omega_1 \ne \omega_2$. For parameter values between bifurcation points HH and BD, it has four complex eigenvalues $\rho \pm \omega i$ and $-\rho \pm \omega i$ with non-zero real part ($\rho \ne 0$). Finally, in between bifurcation points BD and BT, all eigenvalues are real.

Remark 2.1 1. Since $\bar{\nu}_1 = 0$ at the bifurcation points HBT and BT, $p_\pm = (0, 0, 0, 0)$ is the only equilibrium.

2. Although the linearization at the origin has a double zero eigenvalue for the point BT, it is not a generic Bogdanov-Takens point because the vector field is conservative. In the same way, it occurs at the point HBT, where the linearization at the origin matches with a Hopf-Bogdanov-Takens point. Despite this, it should be notice that these bifurcations are generically unfolded in the original family.

3. As the item above suggests, the notation was chosen based on the type of linearization at the equilibrium point. In this sense, the linearization at p_- is related to a Hopf-Hopf bifurcation at the point HH and to a Belyakov-Devaney bifurcation at the point BD.

As usual, when dealing with limit families, it can be more convenient to consider directional rescalings. Namely, we can take $\bar{\nu}_i = +1$ (or $\bar{\nu}_i = -1$) and $(\bar{\nu}_1, \dots, \bar{\nu}_{i-1}, \bar{\nu}_{i+1}, \dots, \bar{\nu}_n) \in \mathbb{R}^{n-1}$ in (1.1). Bearing in mind the study of (1.2) close to the time-reversible subfamily, we consider a directional rescaling with $\bar{\nu}_1 = -1$ to get the family

$$\begin{cases} \bar{x}_1' = \bar{x}_2, \\ \bar{x}_2' = \bar{x}_3, \\ \bar{x}_3' = \bar{x}_4, \\ \bar{x}_4' = -1 + \bar{\nu}_2\bar{x}_2 + \bar{\nu}_3\bar{x}_3 + \bar{\nu}_4\bar{x}_4 + \bar{x}_1^2, \end{cases} \tag{2.1}$$

with $(\bar{\nu}_2, \bar{\nu}_3, \bar{\nu}_4) \in \mathbb{R}^3$.

Remark 2.2 To obtain a complete picture, directional rescalings with $\bar{\nu}_3 = \pm 1$ may be useful. This means to look at the limit family from the bifurcation points BT and HBT.

To compare with results previously obtained in the literature it is better to translate the equilibrium point $p_- = (-1, 0, 0, 0)$ to the origin and rescale variables and parameters as follows:

$$x_1 = \frac{\bar{x}_1 + 1}{2}, \quad x_2 = \frac{\bar{x}_2}{2^{5/4}}, \quad x_3 = \frac{\bar{x}_3}{2^{3/2}}, \quad x_4 = \frac{\bar{x}_4}{2^{7/4}}, \qquad \eta_2 = \frac{\bar{\nu}_2}{2^{3/4}}, \quad \eta_3 = \frac{\bar{\nu}_3}{2^{1/2}}, \quad \eta_4 = \frac{\bar{\nu}_4}{2^{1/4}},$$

to obtain the expression:

$$\begin{cases} x_1' = x_2, \\ x_2' = x_3, \\ x_3' = x_4, \\ x_4' = -x_1 + \eta_2 x_2 + \eta_3 x_3 + \eta_4 x_4 + x_1^2, \end{cases} \tag{2.2}$$

after division by $2^{1/4}$. As already explained, we only have to study the dynamics of system (2.2) around the origin varying $(\eta_2, \eta_3, \eta_4) \in \mathbb{R}^3$ with $\eta_4 \leqslant 0$.

In system (2.2), we first restrict parameters to the reversibility set:

$$\mathcal{T} = \left\{(\eta_2, \eta_3, \eta_4) \in \mathbb{R}^3 \mid \eta_2 = \eta_4 = 0\right\}$$

which, taking $u = x_1$ and $P = -\eta_3$, is equivalent to the fourth order ODE:

$$u^{(4)} + Pu'' + u - u^2 = 0. \tag{2.3}$$

This ODE arises, for instance, in applications to elasticity or fluid problems, and has been widely studied [4–6]. In this case, (2.3) can be expressed by means of Hamilton's equations with Hamiltonian [4]:

$$H = \frac{1}{2}x_1^2 - \frac{1}{3}x_1^3 - \frac{\eta_3}{2}x_2^2 + x_2 x_4 - \frac{1}{2}x_3^2. \tag{2.4}$$

At the same time, (2.3) is a time-reversible system, with reversor:

$$R(x_1, x_2, x_3, x_4) = (x_1, -x_2, x_3, -x_4)$$

such that $R \circ \phi_t = \phi_{-t} \circ R$, being ϕ_t the flow associated to (2.3). When $P < 2$, the origin is an hyperbolic stationary solution, meanwhile it is non-hyperbolic for $P \geqslant 2$. The point $P = 2$ (respectively, $P = -2$) corresponds to the bifurcation point HH (respectively, BD).

We have reproduced numerically some findings of previous works concerning homoclinic orbits of (2.3). The set

$$\mathrm{Fix}(R) = \left\{(x_1, x_2, x_3, x_4) \in \mathbb{R}^4 \mid x_2 = x_4 = 0\right\}$$

plays an important role in their computation. Note that in the hyperbolic case ($P < 2$), when one of the invariant manifolds

$$W^s(0) = \left\{x \in \mathbb{R}^4 \mid \lim_{t\to\infty} \phi_t(x) = 0\right\} \quad \text{or} \quad W^u(0) = \left\{x \in \mathbb{R}^4 \mid \lim_{t\to-\infty} \phi_t(x) = 0\right\}$$

intersects transversally $\mathrm{Fix}(R)$ at x_0, the orbit through x_0 is homoclinic to the origin [6]. We use this property to locate homoclinic trajectories. We describe below the numerical procedures.

3. Numerical approach

3.1. Numerical integration

Equation (2.3), or more generally system (2.2), is integrated in time by means of Taylor method [16]. We apply it by restricting errors bellow 10^{-15}, which consequently impose the order of the Taylor polynomial used in every time step. In the reversible case (2.3), H in (2.4) is a conserved quantity. We use this fact as a test for the numerical integration. In addition, homoclinic orbits belong to the set of zero energy, $\{H = 0\}$, since $H(0) = 0$.

Another important fact is the selection of a proper Poincaré section, in order to classify orbits. We choose $\Sigma = \{x_2 = 0\}$ as the main Poincaré section in our computations.

3.2. Invariant manifolds approximation

In the reversible equation (2.3), $R(W^s(0)) = W^u(0)$ and $\dim(W^u(0)) = \dim(W^s(0)) = 2$ hold for $P < 2$ (see [6]). In the general system (2.2), we still have $\dim(W^u(0)) = \dim(W^s(0)) = 2$ for (η_2, η_3, η_4) close to the line $\{(0, \eta_3, 0) \mid \eta_3 > -2\}$. For this reason, we can consider each of the invariant manifolds, say W, expressed as follows

$$W = \left\{(x_1, x_2, x_3, x_4) \in \mathbb{R}^4 \mid x_3 = a(x_1, x_2), x_4 = b(x_1, x_2)\right\}$$

for certain unknown functions, a and b, smooth enough. We use the Taylor's expansion in power series around the origin:

$$x_3 = \sum_{M=1}^{\infty} \sum_{i=0}^{M} a_{M-i,i} x_1^{M-i} x_2^i \qquad \text{and} \qquad x_4 = \sum_{M=1}^{\infty} \sum_{i=0}^{M} b_{M-i,i} x_1^{M-i} x_2^i \tag{3.1}$$

where $a_{M-i,i}, b_{M-i,i}$ are coefficients corresponding to degree M, to be determined. As W is an invariant manifold, we can impose (3.1) to satisfy system (2.2). With standard but lengthy computations, we obtain a $2(M+1)\times 2(M+1)$ system in the unknowns $a_{M-s,s}, b_{M-s,s}$, for each $M = 1, 2, \dots$ and $s = 0, 1, \dots, M$:

$$\begin{cases} \sum_{k=1}^{M} a_{k-1,1} a_{M-k+1,0} = b_{M,0} & \\ (M - s + 1) a_{M-s+1,s-1} + c_{M-s,s} = b_{M-s,s} & s = 1, \dots, M \\ \sum_{k=1}^{M} b_{k-1,1} a_{M-k+1,0} = \eta_3 a_{M,0} + \eta_4 b_{M,0} - \delta_{M1} + \delta_{M2} & \\ (M - s + 1) b_{M-s+1,s-1} + d_{M-s,s} = \eta_3 a_{M-s,s} + \eta_4 b_{M-s,s} + \eta_2 \delta_{Ms1} & s = 1, \dots, M \end{cases} \tag{3.2}$$

with

$$c_{M-s,s} = \sum_{k=1}^{M} \sum_{i=l_k}^{L_k} i a_{k-i,i} a_{M-k+i-s,s+1-i} \quad \text{and} \quad d_{M-s,s} = \sum_{k=1}^{M} \sum_{i=l_k}^{L_k} i b_{k-i,i} a_{M-k+i-s,s+1-i}$$

where $l_k = \max\{s + k - M, 1\}$, $L_k = \min\{s + 1, k\}$ and $\delta_{xy} = \delta_{xyz} = 1$ only when $x = y = z$ but 0 otherwise. Those systems are solved in increasing order for $M = 1, 2, \dots$. Once we compute $a_{M-s,s}$ and $b_{M-s,s}$, we can only evaluate (3.1) on a certain disk of convergence centered at $(0, 0)$, in the plane defined by (x_1, x_2). Accordingly, in order to approximate a point in an invariant manifold W, we fix (x_1, x_2) not very distant to $(0, 0)$. Using the series (3.1) up to a certain order M, we finally find x_3 and x_4 such that $(x_1, x_2, x_3, x_4) \in W$, up to the truncation error.

4. Time-reversible case

In this section we restrict our study to the time-reversible case, i.e. $\eta_2 = \eta_4 = 0, \eta_3 \in \mathbb{R}$ in (2.2). We apply the tools described above, namely: numerical integrator for system (2.2) and approximation of the invariant manifolds W at the origin. Because W is invariant by the flow ϕ_t, an orbit Γ is included in W, provided there exists $x_0 \in \Gamma \cap W$. By means of the Taylor series (3.1), we approximate $x_0 = (x_1^0, x_2^0, a(x_1^0, x_2^0), b(x_1^0, x_2^0)) \in W$ (with a and b defined in the above section) and, using the numerical integrator, we estimate $\Gamma(x_0)$. In Figure 1, we represent different orbits $\Gamma(x_0(\theta))$ for

$$x_0(\theta) = (x_1, x_2, a(x_1, x_2), b(x_1, x_2)), \quad x_1 = r\cos\theta, \quad x_2 = r\sin\theta, \quad \theta \in [0, 2\pi), \quad \text{and} \quad r = 1/10. \tag{4.1}$$

The value of r is chosen so that series (3.1) are convergent. In fact, the system (3.2) for $M = 1$ gives rise to two solutions corresponding, respectively, to the stable and unstable manifolds.

Homoclinic solutions for ODE (2.3) were analyzed in [4–6]. As stated in the final part of §2, homoclinic orbits corresponds to trajectories with a point in $\mathrm{Fix}(R) \cap W$. In order to find an orbit $\Gamma \subset W$ such that $\Gamma \cap \mathrm{Fix}(R) \neq \emptyset$, we consider initial conditions $x_0(\theta)$ as in (4.1). First, we find $t = t(\theta)$ so that $\phi_t(x_0(\theta)) = (x_1, x_2, x_3, x_4)(\theta, t)$ crosses the Poincaré section $\Sigma = \{x_2 = 0\}$ for a fixed number of times, k. If $x_4(\theta, t) = 0$, then $\phi_t(x_0(\theta)) \in \mathrm{Fix}(R)$ and the orbit through $x_0(\theta)$ is homoclinic. Otherwise, we apply a secant method on θ to vanish $x_4(\theta, t(\theta))$. In Figure 2, we

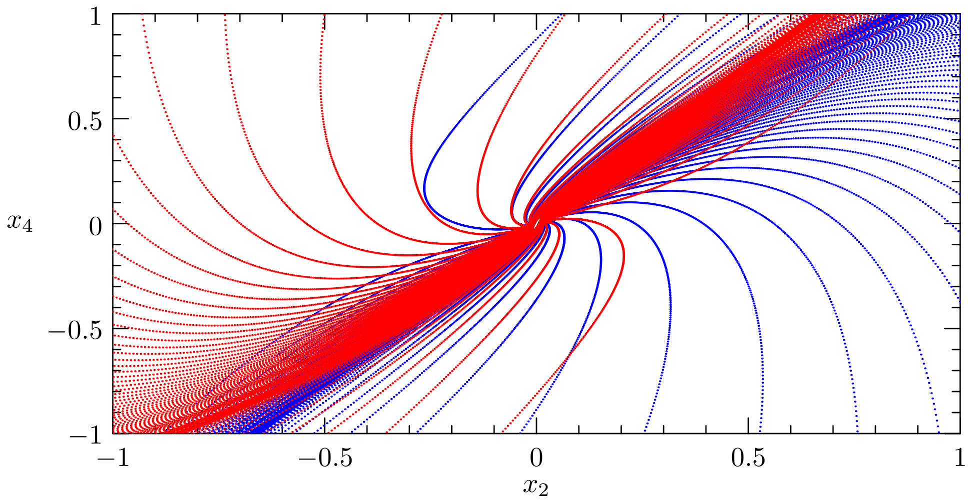

Fig. 1 Different orbits in family (2.2) which make up the stable (blue) and unstable (red) invariant manifolds, close to the origin for $\eta_3 = 1.8$ and projected on the plane (x_2, x_4).

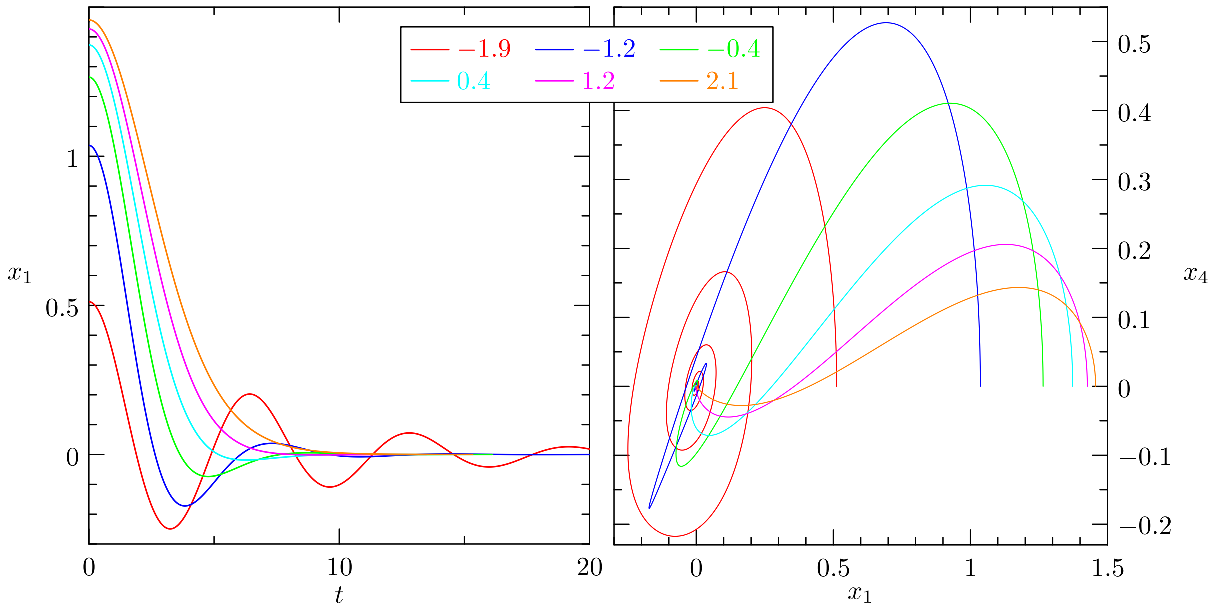

Fig. 2 Homoclinic orbits in family (2.2) for values of η_3 specified by colors. Each orbit starts at $\mathrm{Fix}(R)$ for $t = 0$. Half of the orbit is missing by symmetry. For a given color, different coordinates of the same orbit are shown on the left and right plots. Points in the vertical axis ($t = 0$) on the left panel are in correspondence with points on $x_4 = 0$ on the right panel.

present different homoclinic orbits varying $\eta_3 \in [-1.9, 2.1]$, for $k = 1$. Since we are in the time-reversible case, we have $R \circ \phi_t = \phi_{-t} \circ R$. If the initial condition $\bar{x}_0 \in \mathrm{Fix}(R)$, then:

$$R\phi_t(\bar{x}_0) = \phi_{-t}(R(\bar{x}_0)) = \phi_{-t}(\bar{x}_0)$$

and the orbit is R-symmetric. For this reason, we only plot values for $t \geqslant 0$ in Figure 2.

To improve the plot of the invariant manifolds in Figure 1, we present the curve $W^u(0) \cap \Sigma$ in Figure 3 (left). Each intersection of this curve with $\mathrm{Fix}(R)$ (in red) leads to a homoclinic orbit, which is represented in Figure 3 (right). Particularly, the 11 depicted homoclinic orbits cross Σ a variable number $k = 1, \dots, 5$ of times. The findings for these homoclinics may not be exhaustive, but they give an idea of the dynamics complexity.

All the homoclinic orbits in the time-reversible case belong to the hypersurface $\{H = 0\}$. Taking initial conditions $x_0 \notin \{H = 0\}$, it is not difficult to meet another kind of invariant orbits. For instance, we obtain the solutions plotted in Figure 4 which correspond to invariant tori.

5. Insights in the non-zero divergence case

In the above section, we have analyzed numerically part of the homoclinic phenomena arising in family (2.2) when $\eta_2 = \eta_4 = 0$. In particular, we used the Taylor integrator and the expansion of the invariant manifolds that we

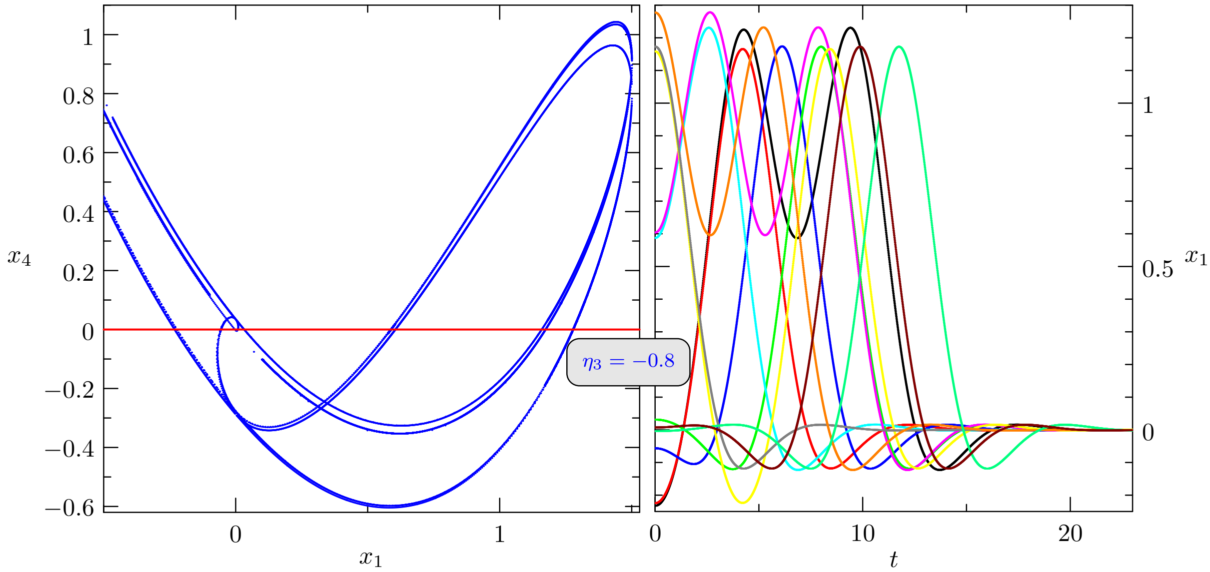

Fig. 3 Invariant manifolds and homoclinic orbits in family (2.2). Left: Curve $W^u(0) \cap \Sigma$ projected on the plane (x_1, x_4). The red line depicts $\mathrm{Fix}(R)$. Right: 11 different homoclinic orbits starting at the respective initial conditions on $W^u(0) \cap \mathrm{Fix}(R)$, located in the left figure as crosses with $\mathrm{Fix}(R)$.

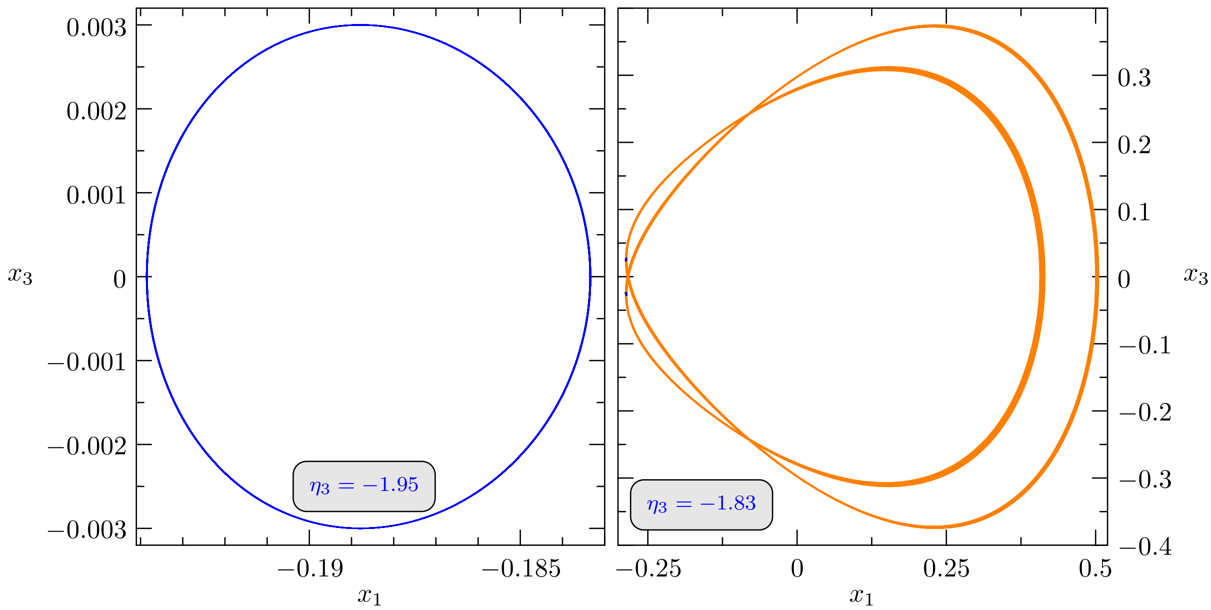

Fig. 4 Quasiperiodic orbits close to periodic, represented on the (x_1, x_3) plane, for family (2.2). Left: Each point of the orbit is only plotted when it crosses Σ. Right: The whole orbit at discrete time values is represented. As a reference, Σ is likewise in this plot, traced on its left side as two little blue curves.

designed specifically for this model. To study the bifurcation diagram around that axis, we can also use numerical continuation methods.

A first overview of the bifurcation complexity is shown in the two bifurcation diagrams in Figure 5, that we obtained using MATCONT [7]. For this analysis, we fix $\bar{\nu}_3 = -3$ and $\bar{\nu}_2 = -0.6$ in family (2.1) and find a Hopf bifurcation at $p_- = (-1, 0, 0, 0)$ when $\bar{\nu}_4 = -0.3$. The continuation of the limit cycle arising at p_- is shown in Figure 5 (left panel, at the bottom). First, an attracting limit cycle emerges from the Hopf bifurcation and loses its stability at a period doubling bifurcation. The periodic orbit recovers stability through another period doubling bifurcation, but loses stability again at a Neimark-Sacker bifurcation where an attracting invariant torus emerges. Finally, the limit cycle disappears at a Hopf bifurcation which occurs at the other equilibrium point $p_+ = (+1, 0, 0, 0)$.

The Hopf bifurcation curve occurring at p_- and the continuation of the Neimark-Sacker bifurcation are represented in Figure 5 (right). Above all, both period doubling bifurcation points belong to the same bifurcation curve, as depicted in Figure 5 (right) where we show a solid red line consisting of two loops.

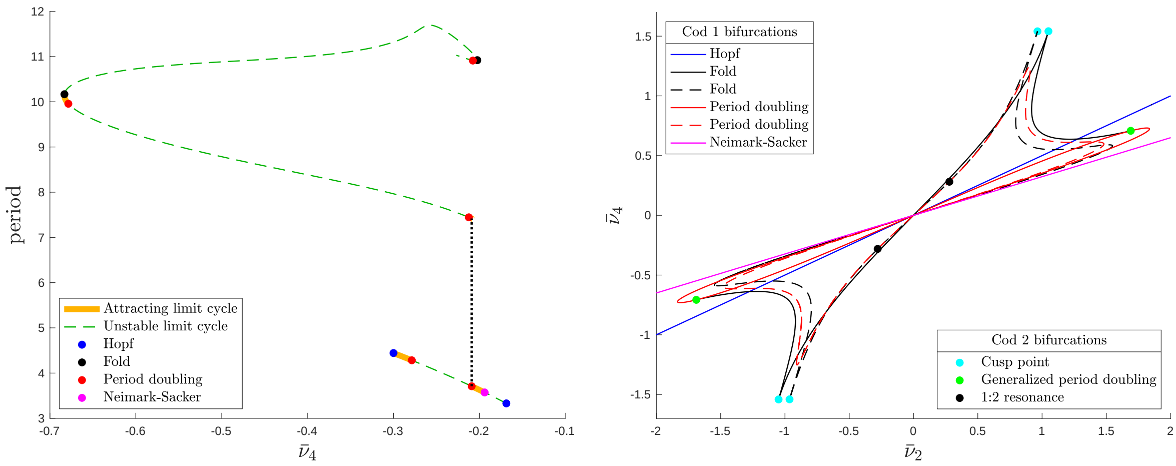

Fig. 5 Left: Continuation of periodic orbits in family (2.1) with $\bar{\nu}_3 = -3$ and $\bar{\nu}_2 = -0.6$. On the one hand, continuation of a periodic orbit emerging from a Hopf bifurcation when $\bar{\nu}_4 = -0.3$ (at the bottom). On the other hand, continuation of a periodic orbit emerging at a period doubling bifurcation (at the top). Right: Partial bifurcation diagram of family (2.1) with $\bar{\nu}_3 = -3$ fixed.

In Figure 5 (left panel, at the top), we also show the continuation of the limit cycle with doubled period that emerges from the period doubling bifurcation point placed on the right side of the continuation curve at the bottom. The attracting limit cycle loses its stability almost immediately due to a period doubling bifurcation. Along the curve we see two fold bifurcation points (black) which belong to the double loop bifurcation curve displayed in Figure 5 (right panel, dashed black line). The limit cycle in between the fold points and the period doubling bifurcation points closer to them is an attractor. These two period doubling points belong to the double loop shown in Figure 5 (right panel, dashed red line).

Additionally, Figure 5 (right) includes a fold bifurcation curve that joins two generalized period doubling bifurcation points (green). Other codimension-two points are the cusp bifurcations of periodic orbits (cyan) and the two point of resonance 1 : 2 (black). A description of the bifurcations mentioned can be found in [17].

6. Discussion

In conclusion, there exist thorough studies [4–6] regarding the complex tangle of homoclinic orbits exhibited by system (2.2) when $\eta_2 = \eta_4 = 0$. Nevertheless, an exhaustive picture is not yet available (see conjectures in [5]). Numerical techniques, which we take advantage of to explore the intersections of the invariant manifolds with a transverse section, are tools that, perhaps for technical reasons, have not been fully exploited in the literature. In this case, despite the fact that the scenario is quite different, our numerical study revives an old paper [18] where the heteroclinic connections unfolded in a reversible three-dimensional system with two equilibrium points of saddle-focus type and different stability indices were studied. Ultimately, the analysis of the traces left by invariant manifolds in a cross section is our most immediate interest. Techniques used in [15] to study Poincaré return maps around a homoclinic orbit to bifocus equilibrium will be useful to describe the geometry of such intersections.

Beyond the homoclinic framework, it is fundamental to analyze the conservative dynamics. In particular, the one that emerges in family (2.2) when $\eta_2 = \eta_4 = 0$ and $\eta_3 < -2$, that is, when the equilibrium point $p_- = (-1, 0, 0, 0)$ is a Hopf-Hopf singularity. In this context, it is also crucial to delve into the dynamics of the family around the point HBT as well as in the surroundings of the point HH. However, these are longer-term goals. In fact, the study of generic unfoldings of Hopf-Bogdanov-Takens singularities has started very recently [9, 10]. Furthermover, we must recall that the limit family is not a generic unfolding of the HBT singularity. The process of reaching a complete theoretical support seems too involved and long. Therefore, all the information that we can collect with continuation tools such as those illustrated in this study will be very useful.

Acknowledgements

The authors has been partially supported by the project MINECO-18-MTM2017-87697-P.

References

[1] P. G. Barrientos, S. Ibáñez and J. A. Rodríguez. Heteroclinic cycles arising in generic unfoldings of nilpotent singularities. *Journal of Dynamics and Differential Equations*, 23(4):999–1028, 2011.

[2] P. G. Barrientos, S. Ibáñez and J. A. Rodríguez. Robust cycles unfolding from conservative bifocal homoclinic orbits. *Dynamical Systems*, 31(4):546–579, 2016.

[3] R. I. Bogdanov. The versal deformation of a singular point of a vector field on the plane in the case of zero eigenvalues. *Trudy Sem. Petrovsky*, 2:37–65, 1976.

[4] B. Buffoni, A. R. Champneys and J. F. Toland. Bifurcation and coalescence of a plethora of homoclinic orbits for a hamiltonian system. *Journal of Dynamics and Differential Equations*, 8(2):221–279, 1996.

[5] A. R. Champneys and J. F. Toland. Bifurcation of a plethora of multi-modal homoclinic orbits for autonomous hamiltonian systems. *Nonlinearity*, 6(5):665–721, 1993.

[6] A. R. Champneys and A. Spence. Hunting for homoclinic orbits in reversible systems: a shooting technique. *Advances in Computational Mathematics*, 1(1):81–108, 1993.

[7] A. Dhooge, W. Govaerts, Yu. A. Kuznetsov, H. G. E. Meijer and B. Sautois. New features of the software MatCont for bifurcation analysis of dynamical systems. *Mathematical and Computer Modelling of Dynamical Systems*, 14(2):147–175, 2008.

[8] F. Drubi, S. Ibáñez and J. A. Rodríguez. Coupling leads to chaos. *Journal of Differential Equations*, 239(2):371–385, 2007.

[9] F. Drubi, S. Ibáñez and D. Rivela. A formal classification of Hopf-Bogdanov-Takens singularities of codimension three. *Journal of Mathematical Analysis and Applications*, 480(2):123408, 2019.

[10] F. Drubi, S. Ibáñez and D. Rivela. Chaotic behavior in the unfolding of Hopf-Bogdanov-Takens singularities. *Discrete and Continuous Dynamical Systems - Series B*, 25(2):599–615, 2020.

[11] F. Dumortier, and S. Ibáñez. Nilpotent singularities in generic 4-parameter families of 3- dimensional vector fields. *Journal of Differential Equations*, 127(2):590–647, 1996.

[12] F. Dumortier, S. Ibáñez and H. Kokubu. New aspects in the unfolding of the nilpotent singularity of codimension three. *Dynamical Systems*, 16(1):63–95, 2001.

[13] F. Dumortier, S. Ibáñez and H. Kokubu. Cocoon bifurcation in three-dimensional reversible vector fields *Nonlinearity*, 19(2):305–328, 2006.

[14] S. Ibáñez and J. A. Rodríguez. Shil'nikov configurations in any generic unfolding of the nilpotent singularity of codimension three on $\mathbb{R}^3$. *Journal of Differential Equations*, 208(1):147–175, 2005.

[15] S. Ibáñez and A. Rodrigues. On the dynamics near a homoclinic network to a bifocus: switching and horseshoes. *International Journal of Bifurcation and Chaos*, 25(11):1530030, 2015.

[16] A. Jorba and M. Zou. A software package for the numerical integration of odes by means of high-order taylor methods. *Experimental Mathematics*, 14(1):99–117, 2005.

[17] Y. Kuznetsov. Elements of Applied Bifurcation Theory. *Applied Mathematical Sciences*, 112, Springer-Verlag New York 2004.

[18] Y.-T. Lau. The cocoon bifurcation in three.dimensional systems with two fixed points. *International Journal of Bifurcation and Chaos*, 2(3):543–558, 1992.

[19] F. Takens. Singularities of vector fields. *Publications mathématiques de l'I.H.É.S*, 43:47–100, 1974.

[20] F. Takens. Forced oscillations and bifurcations. In Applications of global analysis I, *Comm. Math. Inst. Rijksuniv. Utrecht*, 3:1–59, 1974.